

Discovery of Ligands for TRIM58, a Novel Tissue-Selective E3 Ligase

Klemens Hoegenauer,^{*,‡} Shaojian An, Jake Axford, Christina Benander, Christian Bergsdorf, Josephine Botsch, Suzanne Chau, César Fernández, Scott Gleim, Ulrich Hassiepen, Juerg Hunziker, Emilie Joly, Aramis Keller, Sandra Lopez Romero, Robert Maher, Anne-Sophie Mangold, Craig Mickanin, Manuel Mihalic, Philippe Neuner, Andrew W. Patterson, Francesca Perruccio, Silvio Roggo, Julien Scesa, Martin Schröder, Dojna Shkoza, Binh Thai, Anna Vulpetti, Martin Renatus,[‡] and John S. Reece-Hoyes[‡]



Cite This: *ACS Med. Chem. Lett.* 2023, 14, 1631–1639



Read Online

ACCESS |



Metrics & More



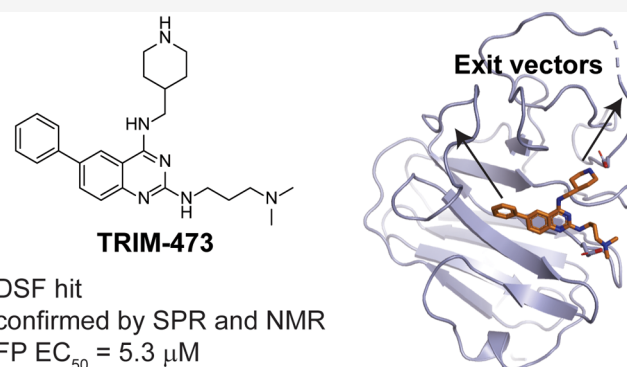
Article Recommendations



Supporting Information

ABSTRACT: Redirecting E3 ligases to neo-substrates, leading to their proteasomal disassembly, known as targeted protein degradation (TPD), has emerged as a promising alternative to traditional, occupancy-driven pharmacology. Although the field has expanded tremendously over the past years, the choice of E3 ligases remains limited, with an almost exclusive focus on CRBN and VHL. Here, we report the discovery of novel ligands to the PRY-SPRY domain of TRIM58, a RING ligase that is specifically expressed in erythroid precursor cells. A DSF screen, followed by validation using additional biophysical methods, led to the identification of TRIM58 ligand **TRIM-473**. A basic SAR around the chemotype was established by utilizing a competitive binding assay employing a short FP peptide probe derived from an endogenous TRIM58 substrate. The X-ray co-crystal structure of TRIM58 in complex with **TRIM-473** gave insights into the binding mode and potential exit vectors for bifunctional degrader design.

KEYWORDS: *targeted protein degradation, RING ligase, PRY-SPRY domain, fluorescent probe design*



Using small molecules to redirect the activity of ubiquitin ligases toward neo-substrates has recently provided new opportunities to target disease-relevant proteins. Their mechanism of action involves recruiting E3 ligases to these proteins (proteins of interest, POIs), leading to polyubiquitination and successively their ubiquitin-mediated proteasomal degradation. This approach is referred to as targeted protein degradation (TPD).¹ The compounds that mediate this mechanism can broadly be divided into two classes: heterobifunctional compounds (also known as proteolysis targeting chimeras, or PROTACs) and molecular glues. Molecular glues function by binding an E3 ligase and inducing a conformational change that enables the ligase to physically interact with a new protein.² The heterobifunctional approach involves synthesizing a compound that is composed of one ligand that binds an E3 ligase tethered to a second ligand that binds the POI, thus inducing proximity and enabling ubiquitination.²

The key for TPD success is a given cellular co-expression profile of the E3 ligase and the target of interest. The first wave of ligases recruited for TPD has been dominated by Cereblon (CRBN) and von Hippel–Lindau tumor suppressor (VHL),³ resulting in several molecules which are being tested in clinical

trials.^{4,5} Both CRBN and VHL are broadly expressed⁶ and thus very useful for degrading a broad range of target proteins in various tissues. However, certain therapeutic approaches could benefit from using E3 ligases with more selective expression patterns to prevent unwanted degradation outside the disease-relevant tissue. Notably, none of the 16 E3 ligases with published TPD activity show selective expression in a particular tissue,^{3,6} yet the fact that VHL is poorly expressed in platelets has been exploited to increase the therapeutic window for BCL-X_L PROTACs.⁷ Of the approximately 600 E3 ligases in the human genome,⁸ many display restricted expression patterns,^{2,9,10} some in tissues that are highly relevant for certain diseases. It is thus reasonable to assume that the next wave of E3 ligases recruited for TPD will focus on

Received: June 12, 2023

Accepted: September 6, 2023

Published: November 13, 2023



higher tissue selectivity to further enhance the safety profiles of TPD-based drugs.

The tripartite motif (TRIM) family of proteins consists of about 80 members, most of which are considered E3 ligases due to the presence of a RING domain, which is a well-known mediator of ubiquitin ligase activity.¹¹ The TRIM family is an untapped resource for TPD, especially for the heterobifunctional approach.^{12,13} TRIM family members exhibit expression patterns useful for degrading a variety of targets, with some expressed broadly while others are expressed selectively in disease-relevant tissues.^{2,9,10} Multiple partial TRIM proteins (but notably none full-length) have been purified and structural data reported, providing solid starting points for ligand identification efforts.¹⁴ To date, only a few ligands for one particular TRIM family member, TRIM24, have been discovered.^{15–17} While no TRIM ligand has been incorporated into a heterobifunctional molecule for driving a TRIM E3 ligase to degrade a neo-substrate, one has been used to generate a heterobifunctional molecule that uses VHL to degrade TRIM24.¹⁸ “TRIM-Away” is a ligand-free approach to degrade antibody-bound POIs in cells and relies on the inherent high affinity of TRIM21 to the Fc domain of antibodies, with apparent therapeutic potential.¹⁹ No other TRIM family member is known to have affinity for the Fc domain, suggesting that the TRIM-Away approach may be unique to the broadly expressed TRIM21.

Both TRIM10 and TRIM58 are exclusively expressed in late-stage erythroblasts,⁹ with demonstrated links to erythrocyte development.^{20–22} Using these E3 ligases for TPD of erythroid-disease-relevant proteins could lead to novel, safer therapies. For example, degrading an HbF repressor protein could lead to novel therapies for sickle cell anemia, as higher HbF levels lead to inconsequential hemolysis and fewer, if any, vaso-occlusive complications. The histone methyl transferases EHMT1 and EMHT2 could be such target proteins, as they are involved in regulating many genes across multiple tissues,^{23,24} and shRNA-mediated knockdown has been shown to increase both HbF synthesis and the number of HbF-expressing cells.²⁵ Leaving EHMT1/2 unaffected in other tissues could avoid potential side effects associated with systemic EHMT1/2 inhibition.²⁶ In contrast to TRIM10, for which no native degradation targets are known, TRIM58 has been shown to degrade multiple targets,^{27–30} notably including the dynein complex during the enucleation step of erythroblast development.³¹ For this reason, we set out to discover ligands for TRIM58 to serve as starting points for erythroblast-specific degradation of HbF repressor proteins.

We expressed and purified several TRIM58^{PRY-SPRY} domain truncation constructs (Figure 1 and Supplementary Figure 1) for a small-molecule screen. The PRY-SPRY domain has been

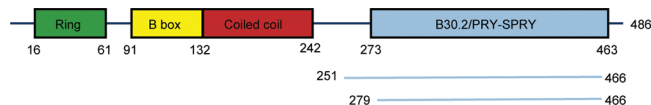


Figure 1. Cartoon representation of the domain architecture of human TRIM58. Numbers below the ring, B-box, coiled-coil, and PRY-SPRY domains represent residue positions of domain boundaries according to Uniprot entry Q8NG06. Lines below the PRY-SPRY domain indicate the boundaries of the proteins used in this study: TRIM58(251–466), TRIM58(251–466)C277S,C278S, and TRIM58(279–466).

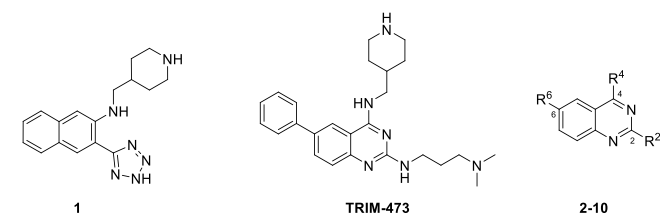
shown in other TRIM family proteins, including murine TRIM58,³¹ to be the physical interface with endogenous target proteins.³² We therefore presumed that generating a heterobifunctional that brought novel targets to this same region of the TRIM58 protein would optimize the chance of such a target being placed in the ubiquitination zone of TRIM58.

To identify binders to the TRIM58^{PRY-SPRY} domain, we used differential scanning fluorimetry (DSF).³³ In our experience, DSF screens require minimal assay development and are especially suited at the onset of projects where a functional assay is not available. Once the first protein batches became available, a diversity set consisting of 45 000 compounds from the Novartis screening deck was tested for binding to TRIM58(251–466) (Figure 1). The structures of primary hits that exhibited dose-dependent stabilization of the protein were used to select similar compounds in the internal archive for subsequent testing by DSF. These compound clusters typically contained several hits that increased the melting temperature of TRIM58(251–466) by 0.5–1.0 °C (data not shown). The most notable cluster, however, was based on an initial hit (compound 1, Table 1) that stabilized TRIM58(251–466) by 0.5–0.7 °C and led to the discovery of TRIM-473 (Table 1), which stabilized the protein by 2.5 °C (Figure 2). This compound was selected for validation in orthogonal biophysical binding assays. In a protein-observed NMR experiment, TRIM-473 induced chemical shift perturbations in the methyl region of 2D [¹³C,¹H]-HMQC spectra recorded with ¹³C,¹⁵N-labeled TRIM58(251–466)C277S,C278S (Figure 2C), indicating that TRIM-473 interacts with TRIM58. In addition, in an SPR binding experiment, TRIM-473 bound to TRIM58(251–466)C277S,C278S with a K_D of 24 μM (Figure 2D).

To further characterize the binding of TRIM-473 to TRIM58, we took advantage of published data about TRIM58 protein targets to develop a competitive binding assay. The PRY-SPRY domain of mouse TRIM58 has been reported to bind the N-terminal 73 residues of dynein intermediate chain (DIC).³¹ We identified the minimal 28-amino-acid peptide of human DIC member DYNC111 that binds the human TRIM58^{PRY-SPRY} domain (Figure 3, Supplementary Figure 2) by testing overlapping sequences for binding in SPR and NMR experiments.

A homology model of a 22-mer DYNC111 peptide binding to TRIM58 was built using the TRIM (258–278) helix as a template (Figure 4C). Although the similarity between the two peptides is only 23%, we hypothesized that the truncated DIC peptide, with a high predicted helical propensity, could bind as observed in the in-house-solved apo TRIM58 structure shown in Figure 4A. The apo structure shows the helical N-terminal portion (259–271) of one TRIM58 chain interacting with a shallow cavity (which later was identified as the TRIM-473 binding site) of the other TRIM58 chain (Figure 4A). The DIC(1–22) peptide model was docked to TRIM58 by locating the L7 side chain at the position occupied by residue L264 of TRIM58 (Figure 4B). This L264 residue is located at a hydrophobic hot spot of the shallow cavity. Based on this model, we assumed Q12 to be solvent exposed (I269, the aligned residue in the TRIM58 chain, is solvent exposed). Replacing this glutamine by a BodipyFL-labeled cysteine in peptide P6 (Figure 3) enabled our fluorescent assay readout, which was further characterized in NMR and SPR experiments (Supplementary Figure 2). We determined that TRIM-473

Table 1. Structure of DSF Hit 1, and Structure–Activity Relationship around TRIM-473



	R ²	R ⁴	R ⁶	TRIM58 FP EC ₅₀ [μM] ^{a, b}	HT-logD ^c	MDCK P _{app} AB ^d	HT-sol [mM] ^e
1	-	-	-	>100	nd	nd	nd
TRIM-473	-	-	-	5.3	<-1.0	0.5	>1.0
2				12	1.1	1.6	0.08
3				8.6	1.2	3.5	0.02
4				>100	-0.5	0.6	>0.75
5				74	1.7	29	>0.75
6				75	2.7		0.10
7				7.4	4.0	19	0.06
8				12.7	3.3	24	0.04
9			H	>100	-0.8	1.6	>0.75
10				6.6	0.5	1.1	>0.75

^aMean of a minimum of two independent experiments; standard deviation for pEC₅₀ values <0.3. ^bCompetitive binding assay (FP) using TRIM58(279–466) protein and the peptidic probe Ac-DKSDLKAELEKCK-C(BODIPY-FL-M)-RLAQIREKKRKEE-NH₂. ^cHigh-throughput logD measurement octanol-buffer (pH = 7.4) based on 96-well shake flask equilibrium and LC/MSMS.³⁸ ^dPermeability coefficient apical-basolateral (P_{app}A-B) in low-efflux Madin–Darby canine kidney cells (MDCK LE).³⁹ ^eHigh-throughput equilibrium solubility determination [mM] (pH = 6.8). nd = not determined.

displaced this fluorescent peptide with an EC₅₀ = 5.3 μM (Table 1), and we were subsequently able to use this assay to determine the TRIM58 binding affinity of various analogs. As TRIM-473 and the labeled truncated endogenous substrate peptide bind to the same area within the TRIM58^{PRY-SPRY} domain, it is likely that functional degraders based on TRIM-

473 would be able to place a neo-substrate within the ubiquitination zone of TRIM58.

For a complete understanding of how TRIM-473 interacts with the TRIM58^{PRY-SPRY} domain, we solved the X-ray structure of the TRIM58(251–466)C277S,C278S/TRIM-473 complex. The TRIM58^{PRY-SPRY} domain adopts a bent β-sandwich fold formed by two antiparallel β-sheets, with TRIM-

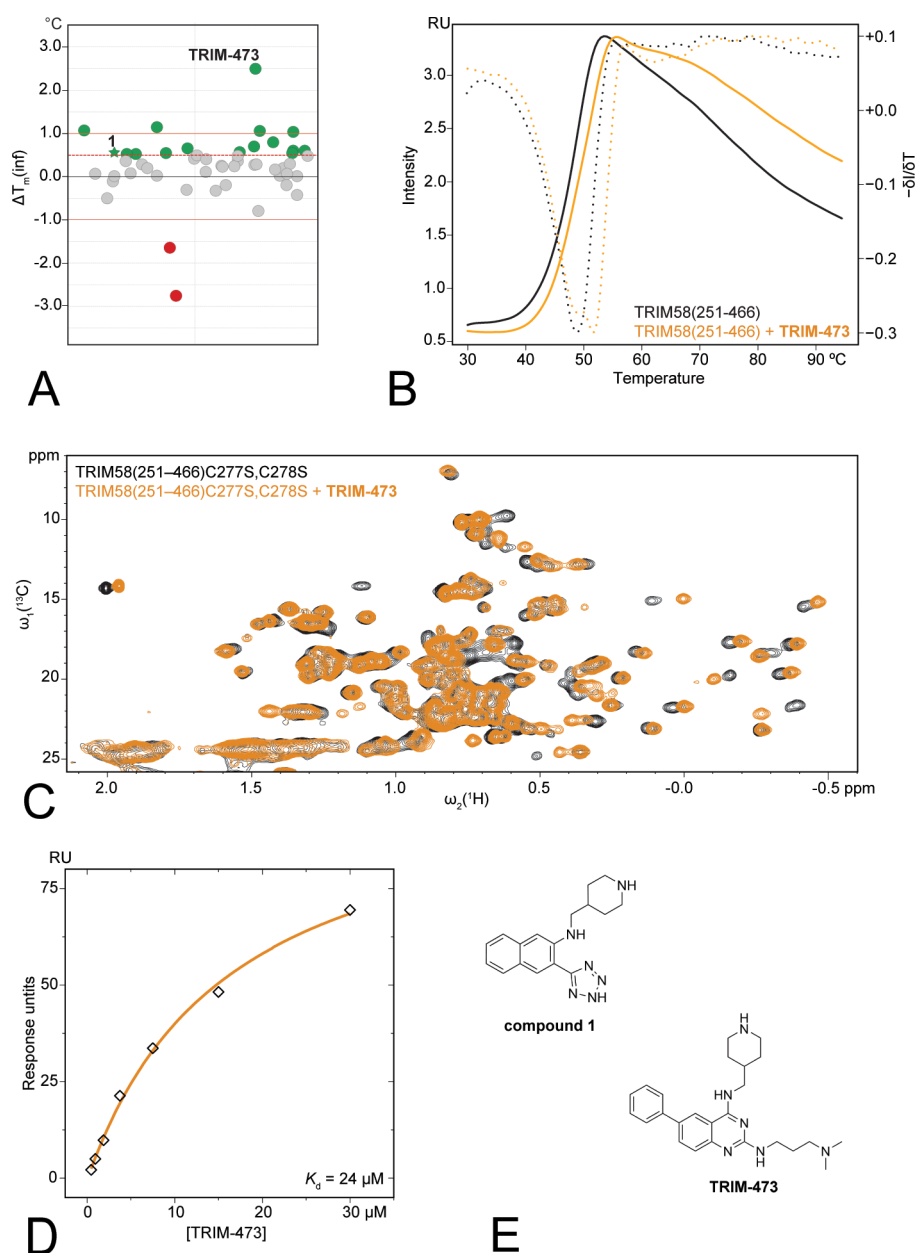


Figure 2. Hit finding and hit validation. A) Shift in transition temperature (ΔT_m) of TRIM58(251–466) observed by DSF experiments with compounds from the hit cluster featuring 107 similar compounds, including TRIM-473. The primary hit for this cluster (compound 1, green star) and TRIM-473 are highlighted. Compounds that lead to a stabilization of $>+0.5$ °C are labeled in green, compounds that lead to a destabilization/stabilization of -1.0 to $+0.5$ °C are labeled in gray, and compounds that lead to a destabilization of <-1 °C are marked in red. B) DSF protein melting curve of TRIM58(251–466) in the presence (orange) and absence (black) of TRIM-473. The dotted curves in gray and orange represent the first derivative of the corresponding protein melting curve. The curve inflection point displays the protein T_m . C) Overlay of the methyl region of 2D $[^{13}\text{C},^1\text{H}]$ -HMQC spectra of uniformly $^{13}\text{C},^{15}\text{N}$ -labeled TRIM58(251–466)C277S,C278S in the absence (black) and in the presence of TRIM-473 (orange), recorded at concentrations of the protein and the compound of 30 and 600 μM , respectively. D) SPR binding experiment for the interaction of TRIM58(251–466)C277S,C278S-Avi with TRIM-473. The equilibrium fit is shown. E) Chemical structures of compounds 1 and TRIM-473.

473 binding an extended surface formed by one of the two β -sheets and the loops connecting its strands (Figure 5A). The quinazoline and the phenyl moieties of the ligand engage in various van der Waals interactions as well as π - π interactions with nearby aromatic side chains (W332, W385, F449). Extended polar interactions (H-bond and ionic) are found between the piperidine-N and the carboxylate of D315, and additionally between the dimethylamino substituent and E357 (Figure 5B). The topology of the binding pocket for TRIM-473 is shallow and hydrophobic (Figure 5C; the area is not

detected as a cavity by standard pocket finder tools, such as the open-source fpocket program or the Site Finder tool in the MOE program), which matches binding pockets mapped for other TRIM family and related ligases.¹⁴

The structure of the TRIM58^{PRY-SPRY} domain aligns well with published experimental structures of the PRY-SPRY domain from other TRIM family members (Figure 6A,B).¹⁴ Additionally, the binding location of TRIM-473 overlaps with published interaction sites for endogenous targets of other TRIM proteins (Figure 6C,D), providing additional evidence

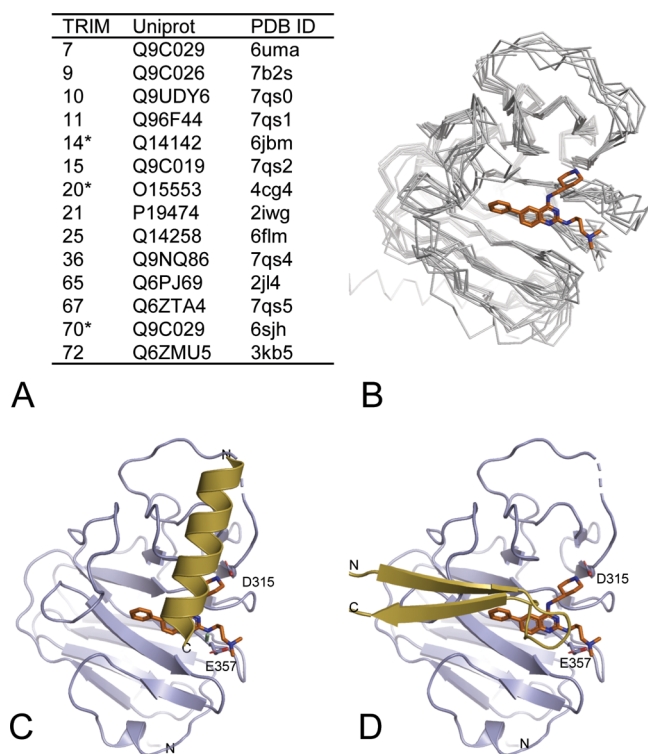


Figure 6. Comparison of the TRIM58^{PRY-SPRY}/TRIM-473 complex structure with those of other TRIM^{PRY-SPRY} domains. A) List of aligned PRY-SPRY domains from 14 human TRIM family proteins. TRIM-like proteins are denoted with an asterisk. B) An overlay of the 14 structures shows that the β -sandwich of two antiparallel β -sheets superimposes well (where TRIM-473 (orange sticks) binds TRIM58), while the loops flanking the substrate binding region diverge significantly. C) Superimposition of the TRIM58^{PRY-SPRY}/TRIM473 complex (gray/orange) with the helical recognition motive of RIG-I (yellow) from the cryo-EM structure of RIG-I:dsRNA filament in complex with RIPLET^{PRY-SPRY} domain (PDG ID: 7JL3).³⁴ D) Superimposition of the TRIM58^{PRY-SPRY}/TRIM473 complex (gray/orange) with the FC domain of IgG (residues 420–443 shown in yellow, PDB ID: 2IWG).³⁵

interactions in this area seem to be more important than the hydrogen bond of the amine, since both compounds bind TRIM58 with EC₅₀ values of 7.4 and 12.7 μ M, respectively. These derivatives are much more lipophilic and therefore less soluble but more permeable. Complete removal of the C6 substituent resulted in an inactive compound **9**. The aromatic C6 substituent could, however, be changed to an aliphatic cyclohexyl ring without activity loss (compound **10**, EC₅₀ = 6.6 μ M). Compared to compound **2**, solubility could be improved due to a lipophilicity drop and an increase in the ratio of sp³-hybridized carbons over the total carbon count of the molecule (fraction Csp³).

Our basic SAR exploration of TRIM-473 suggests that a significant affinity gain toward TRIM58 could be rather difficult to achieve. This is in line with the observation that the ligand is binding a rather shallow surface for which affinity optimization is generally considered more difficult compared to a defined binding pocket.³⁶ Further studies would be necessary to assess whether the current potency range is sufficient for successful degradation. A weak ligase binding K_D can still lead to a highly potent degrader.³⁷ One clear advantage of the shallow binding surface and the solvent-exposed area of the ligand is the multiple promising exit

vectors for bifunctional degrader design, namely, off the C6 phenyl ring or the C4 substituent (Figure 5C).

In summary, we successfully identified ligands for the PRY-SPRY domain of the E3 RING ligase TRIM58 using a DSF screen. We could confirm binding using biophysical techniques, and we developed an FP assay based on truncates of DIC, an endogenous substrate of TRIM58. An X-ray co-crystal structure of TRIM58 with the analog TRIM-473 provided additional evidence that these ligands bind in a shallow area where substrate binding can be expected. Although we were not able to substantially improve the affinity of TRIM-473, we anticipate that our successful ligand identification will encourage follow-up efforts for TRIM58 and other TRIM family ligases, in particular the development of heterobifunctional degraders. Our discoveries expand the toolbox for TPD toward less explored RING ligases and toward ligases with tissue selectivity.

■ ASSOCIATED CONTENT

Supporting Information

The Supporting Information is available free of charge at <https://pubs.acs.org/doi/10.1021/acsmchemlett.3c00259>.

Expression and purification details for protein constructs; full descriptions of all biological assays; synthetic procedures and characterization of all compounds; co-crystallization conditions, crystallographic data collection, and refinement statistics for X-ray crystal structures (PDF)

Accession Codes

X-ray crystal structures described in this study have been deposited in the Protein Data Bank under the following accession codes: PDB ID: 8PD4 (Apo structure of TRIM58-(251–466)C277S,C278S) and PDB ID: 8PD6 (TRIM-473 in complex with TRIM58(251–466)C277S,C278S).

■ AUTHOR INFORMATION

Corresponding Author

Klemens Hoegenauer – Global Discovery Chemistry, Novartis Institutes for BioMedical Research, Novartis Campus, CH-4002 Basel, Switzerland; orcid.org/0000-0001-7266-0137; Phone: (+41) 79 6181814; Email: klemens.hoegenauer@novartis.com

Authors

Shaojian An – Chemical Biology and Therapeutics, Novartis Institutes for BioMedical Research, Cambridge, Massachusetts 02139, United States

Jake Axford – Global Discovery Chemistry, Novartis Institutes for BioMedical Research, Cambridge, Massachusetts 02139, United States

Christina Benander – Chemical Biology and Therapeutics, Novartis Institutes for BioMedical Research, Cambridge, Massachusetts 02139, United States

Christian Bergsdorf – Chemical Biology and Therapeutics, Novartis Institutes for BioMedical Research, Novartis Campus, CH-4002 Basel, Switzerland

Josephine Botsch – Chemical Biology and Therapeutics, Novartis Institutes for BioMedical Research, Novartis Campus, CH-4002 Basel, Switzerland

Suzanne Chau – Chemical Biology and Therapeutics, Novartis Institutes for BioMedical Research, Novartis Campus, CH-4002 Basel, Switzerland

César Fernández – Chemical Biology and Therapeutics, Novartis Institutes for BioMedical Research, Novartis Campus, CH-4002 Basel, Switzerland

Scott Gleim – Chemical Biology and Therapeutics, Novartis Institutes for BioMedical Research, Cambridge, Massachusetts 02139, United States

Ulrich Hassiepen – Chemical Biology and Therapeutics, Novartis Institutes for BioMedical Research, Novartis Campus, CH-4002 Basel, Switzerland

Juerg Hunziker – Global Discovery Chemistry, Novartis Institutes for BioMedical Research, Novartis Campus, CH-4002 Basel, Switzerland

Emilie Joly – Global Discovery Chemistry, Novartis Institutes for BioMedical Research, Novartis Campus, CH-4002 Basel, Switzerland

Aramis Keller – Global Discovery Chemistry, Novartis Institutes for BioMedical Research, Novartis Campus, CH-4002 Basel, Switzerland

Sandra Lopez Romero – Chemical Biology and Therapeutics, Novartis Institutes for BioMedical Research, Novartis Campus, CH-4002 Basel, Switzerland

Robert Maher – Chemical Biology and Therapeutics, Novartis Institutes for BioMedical Research, Cambridge, Massachusetts 02139, United States

Anne-Sophie Mangold – Chemical Biology and Therapeutics, Novartis Institutes for BioMedical Research, Novartis Campus, CH-4002 Basel, Switzerland

Craig Mickanin – Chemical Biology and Therapeutics, Novartis Institutes for BioMedical Research, Cambridge, Massachusetts 02139, United States

Manuel Mihalic – Global Discovery Chemistry, Novartis Institutes for BioMedical Research, Novartis Campus, CH-4002 Basel, Switzerland

Philippe Neuner – Global Discovery Chemistry, Novartis Institutes for BioMedical Research, Novartis Campus, CH-4002 Basel, Switzerland

Andrew W. Patterson – Global Discovery Chemistry, Novartis Institutes for BioMedical Research, Cambridge, Massachusetts 02139, United States

Francesca Perruccio – Global Discovery Chemistry, Novartis Institutes for BioMedical Research, Novartis Campus, CH-4002 Basel, Switzerland

Silvio Roggo – Global Discovery Chemistry, Novartis Institutes for BioMedical Research, Novartis Campus, CH-4002 Basel, Switzerland

Julien Scesa – Global Discovery Chemistry, Novartis Institutes for BioMedical Research, Novartis Campus, CH-4002 Basel, Switzerland

Martin Schröder – Chemical Biology and Therapeutics, Novartis Institutes for BioMedical Research, Novartis Campus, CH-4002 Basel, Switzerland

Dojna Shkoza – Chemical Biology and Therapeutics, Novartis Institutes for BioMedical Research, Cambridge, Massachusetts 02139, United States

Binh Thai – Global Discovery Chemistry, Novartis Institutes for BioMedical Research, Novartis Campus, CH-4002 Basel, Switzerland

Anna Vulpetti – Global Discovery Chemistry, Novartis Institutes for BioMedical Research, Novartis Campus, CH-4002 Basel, Switzerland; orcid.org/0000-0002-3114-8679

Martin Rénatus – Chemical Biology and Therapeutics, Novartis Institutes for BioMedical Research, Novartis

Campus, CH-4002 Basel, Switzerland; Present Address: Ridgeline Discovery, Technologiepark, Hochbergerstr. 60C, CH-4057 Basel, Switzerland

John S. Reece-Hoyes – Chemical Biology and Therapeutics, Novartis Institutes for BioMedical Research, Cambridge, Massachusetts 02139, United States; Present Address: Affina Therapeutics, 43 Foundry Ave., Waltham, MA 02453, USA

Complete contact information is available at: <https://pubs.acs.org/10.1021/acsmmedchemlett.3c00259>

Author Contributions

[‡]K.H., M.R., and J.S.R.-H. contributed equally. C.Ber., S.A., C.Ben., J.B., S.C., C.F., U.H., S.L.R., R.M., A.-S.M., M.S., D.S., M.R., and J.S.R.-H. designed and/or performed biological assays; K.H., J.A., J.H., E.J., A.K., M.M., P.N., A.W.P., F.P., S.R., J.S., B.T., and A.V. designed and synthesized the compounds; S.G. performed bioinformatics analyses; C.M., K.H., M.R., and J.S.R.-H. directed the project; and K.H., M.R. and J.S.R.-H. wrote the manuscript with contributions of all authors.

Notes

The authors declare no competing financial interest.

ACKNOWLEDGMENTS

We thank Felix Freuler and Myriam Duckely for protein expression construct cloning, protein expression, and purification. Deep thanks go to William C. Forrester and Claudio R. Thoma for critical discussions that led to the manuscript in its final form.

ABBREVIATIONS

CRBN, cereblon; DIC, dynein intermediate chain; DSF, differential scanning fluorimetry; FP, fluorescence polarization; SAR, structure–activity relationship; TPD, targeted protein degradation; TRIM, tripartite motif; SPR, surface plasmon resonance; VHL, von Hippel–Lindau tumor suppressor

REFERENCES

- (1) Cowan, A. D.; Ciulli, A. Driving E3 Ligase Substrate Specificity for Targeted Protein Degradation: Lessons from Nature and the Laboratory. *Annu. Rev. Biochem.* **2022**, *91* (1), 295–319.
- (2) Schapira, M.; Calabrese, M. F.; Bullock, A. N.; Crews, C. M. Targeted Protein Degradation: Expanding the Toolbox. *Nat. Rev. Drug Discov* **2019**, *18* (12), 949–963.
- (3) Weng, G.; Shen, C.; Cao, D.; Gao, J.; Dong, X.; He, Q.; Yang, B.; Li, D.; Wu, J.; Hou, T. PROTAC-DB: An Online Database of PROTACs. *Nucleic Acids Res.* **2021**, *49* (D1), D1381–D1387.
- (4) Chirnomas, D.; Hornberger, K. R.; Crews, C. M. Protein Degraders Enter the Clinic — a New Approach to Cancer Therapy. *Nat. Rev. Clin. Oncol* **2023**, *20* (4), 265–278.
- (5) Chen, Y.; Tandon, I.; Heelan, W.; Wang, Y.; Tang, W.; Hu, Q. Proteolysis-Targeting Chimera (PROTAC) Delivery System: Advancing Protein Degradation towards Clinical Translation. *Chem. Soc. Rev.* **2022**, *51* (13), 5330–5350.
- (6) Uhlén, M.; Fagerberg, L.; Hallström, B. M.; Lindskog, C.; Oksvold, P.; Mardinoglu, A.; Sivertsson, Å.; Kampf, C.; Sjöstedt, E.; Asplund, A.; Olsson, I. M.; Edlund, K.; Lundberg, E.; Navani, S.; Szijarto, C. A. K.; Odeberg, J.; Djureinovic, D.; Takanen, J. O.; Hober, S.; Alm, T.; Edqvist, P. H.; Berling, H.; Tegel, H.; Mulder, J.; Rockberg, J.; Nilsson, P.; Schwenk, J. M.; Hamsten, M.; Von Feilitzen, K.; Forsberg, M.; Persson, L.; Johansson, F.; Zwahlen, M.; Von Heijne, G.; Nielsen, J.; Pontén, F. Tissue-Based Map of the Human Proteome. *Science* (1979) **2015**, *347* (6220), 394.

- (7) Khan, S.; Zhang, X.; Lv, D.; Zhang, Q.; He, Y.; Zhang, P.; Liu, X.; Thummuri, D.; Yuan, Y.; Wiegand, J. S.; Pei, J.; Zhang, W.; Sharma, A.; McCurdy, C. R.; Kuruvilla, V. M.; Baran, N.; Ferrando, A. A.; Kim, Y.; Rogojina, A.; Houghton, P. J.; Huang, G.; Hromas, R.; Konopleva, M.; Zheng, G.; Zhou, D. A Selective BCL-XL PROTAC Degradator Achieves Safe and Potent Antitumor Activity. *Nat. Med.* **2019**, *25* (12), 1938–1947.
- (8) Liu, L.; Damerell, D. R.; Koukouflis, L.; Tong, Y.; Marsden, B. D.; Schapira, M. UbiHub: A Data Hub for the Explorers of Ubiquitination Pathways. *Bioinformatics* **2019**, *35* (16), 2882–2884.
- (9) Jevtić, P.; Haakonsen, D. L.; Rapé, M. An E3 Ligase Guide to the Galaxy of Small-Molecule-Induced Protein Degradation. *Cell Chem. Biol.* **2021**, *28* (7), 1000–1013.
- (10) Guenette, R. G.; Yang, S. W.; Min, J.; Pei, B.; Potts, P. R. Target and Tissue Selectivity of PROTAC Degradators. *Chem. Soc. Rev.* **2022**, *51* (14), 5740–5756.
- (11) Hatakeyama, S. TRIM Family Proteins: Roles in Autophagy, Immunity, and Carcinogenesis. *Trends Biochem. Sci.* **2017**, *42*, 297–311.
- (12) Bhaduri, U.; Merla, G. Ubiquitination, Biotech Startups, and the Future of Trim Family Proteins: A Trim-Endous Opportunity. *Cells* **2021**, *10*, 1015.
- (13) D'Amico, F.; Mukhopadhyay, R.; Ovaia, H.; Mulder, M. P. C. Targeting TRIM Proteins: A Quest towards Drugging an Emerging Protein Class. *ChemBioChem.* **2021**, *22* (12), 2011–2031.
- (14) Ishida, T.; Ciulli, A. E3 Ligase Ligands for PROTACs: How They Were Found and How to Discover New Ones. *SLAS Discovery* **2021**, *26* (4), 484–502.
- (15) Bennett, J.; Fedorov, O.; Tallant, C.; Monteiro, O.; Meier, J.; Gamble, V.; Savitsky, P.; Nunez-Alonso, G. A.; Haendler, B.; Rogers, C.; Brennan, P. E.; Müller, S.; Knapp, S. Discovery of a Chemical Tool Inhibitor Targeting the Bromodomains of TRIM24 and BRPF. *J. Med. Chem.* **2016**, *59* (4), 1642–1647.
- (16) Palmer, W. S.; Poncet-Montange, G.; Liu, G.; Petrocchi, A.; Reyna, N.; Subramanian, G.; Theroff, J.; Yau, A.; Kost-Alimova, M.; Bardenhagen, J. P.; Leo, E.; Shepard, H. E.; Tieu, T. N.; Shi, X.; Zhan, Y.; Zhao, S.; Barton, M. C.; Draetta, G.; Toniatti, C.; Jones, P.; Geck Do, M.; Andersen, J. N. Structure-Guided Design of IACS-9571, a Selective High-Affinity Dual TRIM24-BRPF1 Bromodomain Inhibitor. *J. Med. Chem.* **2016**, *59* (4), 1440–1454.
- (17) Hu, Q.; Wang, C.; Xiang, Q.; Wang, R.; Zhang, C.; Zhang, M.; Xue, X.; Luo, G.; Liu, X.; Wu, X.; Zhang, Y.; Wu, D.; Xu, Y. Discovery and Optimization of Novel N-Benzyl-3,6-Dimethylbenzo[d]isoxazol-5-Amine Derivatives as Potent and Selective TRIM24 Bromodomain Inhibitors with Potential Anti-Cancer Activities. *Bioorg Chem.* **2020**, *94*, 103424.
- (18) Gechijian, L. N.; Buckley, D. L.; Lawlor, M. A.; Reyes, J. M.; Paulk, J.; Ott, C. J.; Winter, G. E.; Erb, M. A.; Scott, T. G.; Xu, M.; Seo, H. S.; Dhe-Paganon, S.; Kwiatkowski, N. P.; Perry, J. A.; Qi, J.; Gray, N. S.; Bradner, J. E. Functional TRIM24 Degradator via Conjugation of Ineffective Bromodomain and VHL Ligands Article. *Nat. Chem. Biol.* **2018**, *14* (4), 405–412.
- (19) Benn, J. A.; Mukadam, A. S.; McEwan, W. A. Targeted Protein Degradation Using Intracellular Antibodies and Its Application to Neurodegenerative Disease. *Semin Cell Dev Biol.* **2022**, *126*, 138–149.
- (20) Harada, H.; Harada, Y.; O'Brien, D. P.; Rice, D. S.; Naeve, C. W.; Downing, J. R. HERF1, a Novel Hematopoiesis-Specific RING Finger Protein, Is Required for Terminal Differentiation of Erythroid Cells. *Mol. Cell. Biol.* **1999**, *19* (5), 3808–3815.
- (21) Kamatani, Y.; Matsuda, K.; Okada, Y.; Kubo, M.; Hosono, N.; Daigo, Y.; Nakamura, Y.; Kamatani, N. Genome-Wide Association Study of Hematological and Biochemical Traits in a Japanese Population. *Nat. Genet.* **2010**, *42* (3), 210–215.
- (22) Van Der Harst, P.; Zhang, W.; Mateo Leach, I.; Rendon, A.; Verweij, N.; Sehmi, J.; Paul, D. S.; Elling, U.; Allayee, H.; Li, X.; Radhakrishnan, A.; Tan, S. T.; Voss, K.; Weichenberger, C. X.; Albers, C. A.; Al-Hussani, A.; Asselbergs, F. W.; Ciullo, M.; Danjou, F.; Dina, C.; Esko, T.; Evans, D. M.; Franke, L.; Gögele, M.; Hartiala, J.; Hersch, M.; Holm, H.; Hottenga, J. J.; Kanoni, S.; Kleber, M. E.; Lagou, V.; Langenberg, C.; Lopez, L. M.; Lyytikäinen, L. P.; Melander, O.; Murgia, F.; Nolte, I. M.; O'Reilly, P. F.; Padmanabhan, S.; Parsa, A.; Pirastu, N.; Porcu, E.; Portas, L.; Prokopenko, I.; Ried, J. S.; Shin, S. Y.; Tang, C. S.; Teumer, A.; Traglia, M.; Ulivi, S.; Westra, H. J.; Yang, J.; Hua Zhao, J.; Anni, F.; Abdellaoui, A.; Attwood, A.; Balkau, B.; Bandinelli, S.; Bastardot, F.; Benjamin, B.; Boehm, B. O.; Cookson, W. O.; Das, D.; De Bakker, P. I. W.; De Boer, R. A.; De Geus, E. J. C.; De Moor, M. H.; Dimitriou, M.; Domingues, F. S.; Döring, A.; Engström, G.; Eyjolfsson, G. I.; Ferrucci, L.; Fischer, K.; Galanella, R.; Garner, S. F.; Genser, B.; Gibson, Q. D.; Girotto, G.; Gudbjartsson, D. F.; Harris, S. E.; Hartikainen, A. L.; Hastie, C. E.; Hedblad, B.; Illig, T.; Jolley, J.; Kähönen, M.; Kema, I. P.; Kemp, J. P.; Liang, L.; Lloyd-Jones, H.; Loos, R. J. F.; Meacham, S.; Medland, S. E.; Meisinger, C.; Memari, Y.; Mihailov, E.; Miller, K.; Moffatt, M. F.; Nauck, M.; Novatchkova, M.; Nutile, T.; Olafsson, I.; Onundarson, P. T.; Parracciani, D.; Penninx, B. W.; Perseu, L.; Piga, A.; Pistis, G.; Pouta, A.; Puc, U.; Raitakari, O.; Ring, S. M.; Robino, A.; Ruggiero, D.; Ruokonen, A.; Saint-Pierre, A.; Sala, C.; Salumets, A.; Sambrook, J.; Schepers, H.; Schmidt, C. O.; Silljé, H. H. W.; Sladek, R.; Smit, J. H.; Starr, J. M.; Stephens, J.; Sulem, P.; Tanaka, T.; Thorsteinsdottir, U.; Tragante, V.; Van Gilst, W. H.; Joost Van Pelt, L.; Van Veldhuisen, D. J.; Völker, U.; Whitfield, J. B.; Willemsen, G.; Winkelmann, B. R.; Wirsberger, G.; Algra, A.; Cucca, F.; D'Adamo, A. P.; Danesh, J.; Deary, I. J.; Dominiczak, A. F.; Elliott, P.; Fortina, P.; Froguel, P.; Gasparini, P.; Greinacher, A.; Hazen, S. L.; Jarvelin, M. R.; Khaw, K. T.; Lehtimäki, T.; Maerz, W.; Martin, N. G.; Metspalu, A.; Mitchell, B. D.; Montgomery, G. W.; Moore, C.; Navis, G.; Pirastu, M.; Pramstaller, P. P.; Ramirez-Solis, R.; Schadt, E.; Scott, J.; Shuldiner, A. R.; Smith, G. D.; Gustav Smith, J.; Snieder, H.; Sorice, R.; Spector, T. D.; Stefansson, K.; Stumvoll, M.; Wilson Tang, W. H.; Toniolo, D.; Tönjes, A.; Visscher, P. M.; Vollenweider, P.; Wareham, N. J.; Wolffebuttel, B. H. R.; Boomsma, D. I.; Beckmann, J. S.; Dedoussis, G. V.; Deloukas, P.; Ferreira, M. A.; Sanna, S.; Uda, M.; Hicks, A. A.; Penninger, J. M.; Gieger, C.; Kooner, J. S.; Ouwehand, W. H.; Soranzo, N.; Chambers, J. C. Seventy-Five Genetic Loci Influencing the Human Red Blood Cell. *Nature* **2012**, *492* (7429), 369–375.
- (23) Pangeni, R. P.; Yang, L.; Zhang, K.; Wang, J.; Li, W.; Guo, C.; Yun, X.; Sun, T.; Wang, J.; Raz, D. J. G9a Regulates Tumorigenicity and Stemness through Genome-Wide DNA Methylation Reprogramming in Non-Small Cell Lung Cancer. *Clin Epigenetics* **2020**, *12* (1), 88.
- (24) Papait, R.; Serio, S.; Pagiatakis, C.; Rusconi, F.; Carullo, P.; Mazzola, M.; Salvarani, N.; Miragoli, M.; Condorelli, G. Histone Methyltransferase G9a Is Required for Cardiomyocyte Homeostasis and Hypertrophy. *Circulation* **2017**, *136* (13), 1233–1246.
- (25) Renneville, A.; Van Galen, P.; Canver, M. C.; McConkey, M.; Krill-Burger, J. M.; Dorfman, D. M.; Holson, E. B.; Bernstein, B. E.; Orkin, S. H.; Bauer, D. E.; Ebert, B. L. EHMT1 and EHMT2 Inhibition Induces Fetal Hemoglobin Expression. *Blood* **2015**, *126* (16), 1930–1939.
- (26) Rahman, Z.; Bazaz, M. R.; Devabattula, G.; Khan, M. A.; Godugu, C. Targeting H3K9Methyltransferase G9a and Its Related Molecule GLP as a Potential Therapeutic Strategy for Cancer. *J. Biochem Mol. Toxicol* **2021**, *35* (3), e22674.
- (27) Liu, X.; Long, Z.; Cai, H.; Yu, S.; Wu, J. TRIM58 Suppresses the Tumor Growth in Gastric Cancer by Inactivation of β -Catenin Signaling via Ubiquitination. *Cancer Biol. Ther* **2020**, *21* (3), 203–212.
- (28) Yuan, P.; Zhou, Y.; Wang, R.; Chen, S.; Wang, Q.; Xu, Z.; Liu, Y.; Yang, H. TRIM58 Interacts with Pyruvate Kinase M2 to Inhibit Tumorigenicity in Human Osteosarcoma Cells. *Biomed Res. Int.* **2020**, *2020*, 8450606.
- (29) Eyking, A.; Ferber, F.; Köhler, S.; Reis, H.; Cario, E. TRIM58 Restrains Intestinal Mucosal Inflammation by Negatively Regulating TLR2 in Myeloid Cells. *J. Immunol.* **2019**, *203* (6), 1636–1649.
- (30) Wang, J.; Yang, F.; Zhuang, J.; Huo, Q.; Li, J.; Xie, N. TRIM58 Inactivates P53/P21 to Promote Chemoresistance via Ubiquitination

of DDX3 in Breast Cancer. *Int. J. Biochem. Cell Biol.* **2022**, *143*, 106140.

(31) Thom, C. S.; Traxler, E. A.; Khandros, E.; Nickas, J. M.; Zhou, O. Y.; Lazarus, J. E.; Silva, A. P. G.; Prabhu, D.; Yao, Y.; Aribéana, C.; Fuchs, S. Y.; Mackay, J. P.; Holzbaur, E. L. F.; Weiss, M. J. Trim58 Degrades Dynein and Regulates Terminal Erythropoiesis. *Dev Cell* **2014**, *30* (6), 688–700.

(32) Jumper, J.; Evans, R.; Pritzel, A.; Green, T.; Figurnov, M.; Ronneberger, O.; Tunyasuvunakool, K.; Bates, R.; Žídek, A.; Potapenko, A.; Bridgland, A.; Meyer, C.; Kohl, S. A. A.; Ballard, A. J.; Cowie, A.; Romera-Paredes, B.; Nikolov, S.; Jain, R.; Adler, J.; Back, T.; Petersen, S.; Reiman, D.; Clancy, E.; Zielinski, M.; Steinegger, M.; Pacholska, M.; Berghammer, T.; Bodenstein, S.; Silver, D.; Vinyals, O.; Senior, A. W.; Kavukcuoglu, K.; Kohli, P.; Hassabis, D. Highly Accurate Protein Structure Prediction with AlphaFold. *Nature* **2021**, *596* (7873), 583–589.

(33) Gao, K.; Oerlemans, R.; Groves, M. R. Theory and Applications of Differential Scanning Fluorimetry in Early-Stage Drug Discovery. *Biophys Rev.* **2020**, *12* (1), 85–104.

(34) Kato, K.; Ahmad, S.; Zhu, Z.; Young, J. M.; Mu, X.; Park, S.; Malik, H. S.; Hur, S. Structural Analysis of RIG-I-like Receptors Reveals Ancient Rules of Engagement between Diverse RNA Helicases and TRIM Ubiquitin Ligases. *Mol. Cell* **2021**, *81* (3), 599–613.e8.

(35) James, L. C.; Keeble, A. H.; Khan, Z.; Rhodes, D. A.; Trowsdale, J. Structural Basis for PRYSPRY-Mediated Tripartite Motif (TRIM) Protein Function. *Proc. Natl. Acad. Sci. U. S. A.* **2007**, *104* (15), 6200–6205.

(36) Shin, W.-H.; Kumazawa, K.; Imai, K.; Hirokawa, T.; Kihara, D. Current Challenges and Opportunities in Designing Protein–Protein Interaction Targeted Drugs. *Advances and Applications in Bioinformatics and Chemistry* **2020**, *13*, 11–25.

(37) Testa, A.; Lucas, X.; Castro, G. V.; Chan, K.-H.; Wright, J. E.; Runcie, A. C.; Gadd, M. S.; Harrison, W. T. A.; Ko, E.-J.; Fletcher, D.; Ciulli, A. 3-Fluoro-4-Hydroxyprolines: Synthesis, Conformational Analysis, and Stereoselective Recognition by the VHL E3 Ubiquitin Ligase for Targeted Protein Degradation. *J. Am. Chem. Soc.* **2018**, *140* (29), 9299–9313.

(38) Low, Y. W.; Blasco, F.; Vachaspati, P. Optimised Method to Estimate Octanol Water Distribution Coefficient (LogD) in a High Throughput Format. *European Journal of Pharmaceutical Sciences* **2016**, *92*, 110–116.

(39) Di, L.; Whitney-Pickett, C.; Umland, J. P.; Zhang, H.; Zhang, X.; Gebhard, D. F.; Lai, Y.; Federico, J. J.; Davidson, R. E.; Smith, R.; Reyner, E. L.; Lee, C.; Feng, B.; Rotter, C.; Varma, M. V.; Kempshall, S.; Fenner, K.; El-kattan, A. F.; Liston, T. E.; Troutman, M. D. Development of a New Permeability Assay Using Low-efflux MDCKII Cells. *J. Pharm. Sci.* **2011**, *100* (11), 4974–4985.